 Bull. Chem. Soc. Jpn. Vol. 80, No. 7, 1229–1240 (2007)

Vol. 80 Commemorative Accounts

The Jahn–Teller Effect in Chemistry

Arnout Ceulemans* **and Erwin Lijnen**

Department of Chemistry and INPAC Institute for Nanoscale Physics and Chemistry, Katholieke Universiteit Leuven, Celestijnenlaan 200F, B-3001 Leuven, Belgium

Received February 7, 2007; E-mail: arnout.ceulemans@chem.kuleuven.be

A uniform view of electronic degeneracies, resulting from finite point group symmetries, is developed. It relates any *n*-fold degeneracy to the geometrical structure formed by the set of equidistant points in a space with exactly *n* dimensions. Jahn–Teller interactions within the degenerate manifold can simply be represented as bond stretchings of this structure. This approach thus can be qualified as the "chemical perspective" to the study of vibronic instabilities. The procedure is described for two-fold, three-fold, four-fold, and five-fold degeneracies. As a result a simple general proof of the Jahn–Teller theorem can be obtained. The electronic degeneracy is connected to the reaction graph of the stable minima on the surrounding Jahn–Teller surface. The findings are illustrated with some structural and dynamic molecular examples.

Introduction

Degeneracy occurs whenever a given eigenstate of a system is realized in more than one way. This means that two or more independent eigenfunctions of the Schrödinger equation are associated with the same eigenvalue. This phenomenon is typical for the quantum state of matter and has no analogue in classical systems. Degeneracy can be accidental, as when two states cross at a particular geometry or for a certain value of some external field, but the legal cases are those where degeneracy is due to the presence of space or time symmetries.

It was with the spatial symmetry degeneracies in mind that Jahn and Teller stated in 1937 their remarkable theorem that all non-linear nuclear configurations are unstable for an orbitally degenerate electronic state.[1] The instability will trigger a distortion to a lower symmetry that removes the cause of degeneracy and thus leads to a non-degenerate state. In other words, symmetry and degeneracy do not seem to go together, and nature will always find ways to avoid such situations.[2]

The present account intends to show the common structure which unites all Jahn–Teller (JT) cases and is based on the connection between the point groups and the symmetric groups, describing the permutations of identical particles. The presentation is as much as possible in terms of geometric arguments, and several illustrations from chemical applications are included. The approach starts from the two-fold degeneracy and gradually attains the icosahedral five-fold degeneracy which is the highest case of orbital degeneracy.

Two-Fold Degeneracy: The Triangle

Two-fold orbital degeneracy can be realised most simply in an equilateral triangular structure. Such a structure is also called the simplex of two-dimensional space, i.e. a structure in which all atoms are equidistant. In 2D space, only three points can be perfectly equidistant from each other, so in a way, the triangle forms the basic building block of the plane, as is illustrated by the triangular tessellation of the plane. If one would consider four points in a plane, it is already impossible to find a configuration for which they are all at the same distance from each other.

The symmetry group of the simplex is the group of all possible permutations of its vertices. For *n* vertices, this group is called the symmetric group of order *n*, S_n, and its number of elements is *n*! In the case of a triangle, there are six possible permutations of the three constituent nuclei, forming the group S_3, which is isomorphic to the point group C_{3v}. This is also the smallest point group with a two-fold degenerate representation, and it therefore represents the simplest example of a JT effect.

The JT activity in this case can very easily be derived by considering a straightforward basis set, only consisting of s-type functions on the vertices of the triangle, such as in a triangle of three hydrogenic atoms.[3] We will elaborate this simple case in some detail, since the same procedure as used here will be found to be applicable to all higher degeneracy cases. With the three basis functions of the triangle, two types of molecular orbitals can be formed, transforming as a_1 and e:

$$\psi_{a_1} = \frac{1}{\sqrt{3}}(\varphi_1 + \varphi_2 + \varphi_3).$$
$$\psi_{e\vartheta} = \frac{1}{\sqrt{6}}(2\varphi_1 - \varphi_2 - \varphi_3).$$
$$\psi_{e\varepsilon} = \frac{1}{\sqrt{2}}(\varphi_3 - \varphi_2). \quad (1)$$

Published on the web July 11, 2007; doi:10.1246/bcsj.80.1229

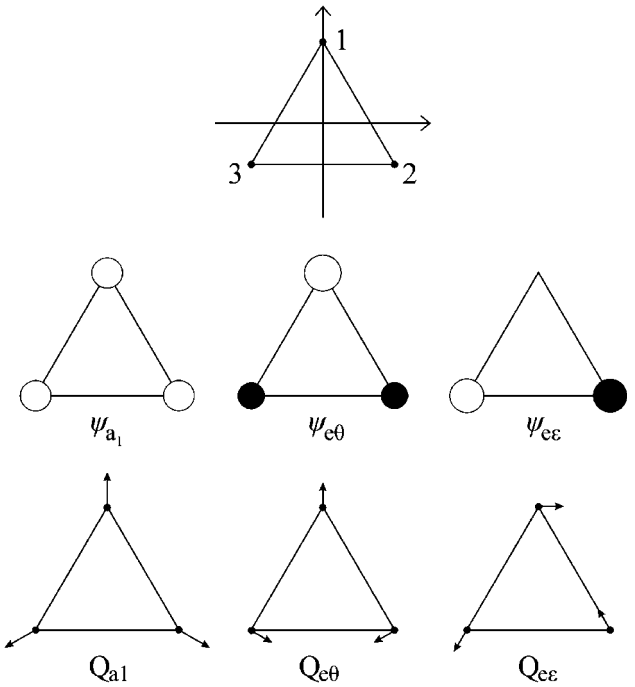

Fig. 1. The two-fold degeneracy and the triangle: basic structure, orbital basis, and the normal modes corresponding to edge stretchings. The ψ_e-orbital basis is JT active under the Q_e-modes.

These orbitals are represented in the Fig. 1. The two e-components are labeled with the indices θ and ε, and are resp. symmetric and antisymmetric with respect to a vertical symmetry plane through atom 1. If the ground state of the triangle would be realised by occupying only the totally symmetric a_1 orbital with one or two electrons, it is clear that the total charge density would also be totally symmetric. Hence, in this case, the distribution of the nuclei which are the origins of the positive charges in the molecule, and the electron density cloud, which carries the negative-charge distribution, are both symmetrical, and there cannot be electric forces between the two charge distributions that will lead to spontaneous symmetry lowering distortions. In general, any non-degenerate eigenfunction is either symmetrical or antisymmetrical under the symmetry transformations of the molecular point group, so that the charge density, expressed as the square of the wave function, will always be symmetrical. As a result, for non-degenerate ground states, there is no spontaneous symmetry breaking.

If, however, the orbitally degenerate e-level is occupied by a single electron, the situation is more complicated. Instead of one wave function, we now have two wave functions, spanning the two-dimensional irreducible representation of the C_{3v} molecular point group. Instead of the usual charge density cloud, such a state is now characterised by a 2×2 density matrix. The electronic energies may most simply be expressed by a Hamiltonian matrix in the two-dimensional orbital space. The bonding interactions are due to the exchange integrals of type $\langle\varphi_i|H|\varphi_j\rangle$. We will adopt the simple model in which these integrals are a linear function of the bond lengths separating atoms i and j. Since all atoms are equidistant, we can introduce a common slope k:

$$\langle\varphi_i|H|\varphi_j\rangle = k\Delta r_{ij}. \tag{2}$$

We may express this result in an operator form as follows:

$$H = \sum_{k<l} k\Delta r_{kl}(|\varphi_k\rangle\langle\varphi_l| + |\varphi_l\rangle\langle\varphi_k|). \tag{3}$$

The Hamiltonian matrix which results from this parametrization is easily derived using the orbital expressions in Eq. 1.

$$H = k \times \begin{pmatrix} \frac{2}{3}(\Delta r_{12} + \Delta r_{13} + \Delta r_{23}) & \frac{1}{3\sqrt{2}}(\Delta r_{12} + \Delta r_{13} - 2\Delta r_{23}) & \frac{1}{\sqrt{6}}(\Delta r_{13} - \Delta r_{12}) \\ \frac{1}{3\sqrt{2}}(\Delta r_{12} + \Delta r_{13} - 2\Delta r_{23}) & \frac{1}{3}(-2\Delta r_{12} - 2\Delta r_{13} + \Delta r_{23}) & \frac{1}{\sqrt{3}}(\Delta r_{13} - \Delta r_{12}) \\ \frac{1}{\sqrt{6}}(\Delta r_{13} - \Delta r_{12}) & \frac{1}{\sqrt{3}}(\Delta r_{13} - \Delta r_{12}) & -\Delta r_{23} \end{pmatrix}. \tag{4}$$

Here, we have ordered the basis orbitals as $\{a_1, e\theta, e\varepsilon\}$. The symmetry transformations of the nuclei also will act transitively on the three bond lengths of our triangle, since these are simple pairfunctions of the nuclei. Note that they are even functions of the bond pair, hence a permutation of the nuclei i and j along a common bond will leave the distance unchanged, i.e.:

$$P_{ij}\Delta r_{ij} = \Delta r_{ij}. \tag{5}$$

As a result, the coordinates can be regrouped into symmetry adapted normal coordinates. One obtains one totally symmetric or breathing mode, and two asymmetric e-type stretching components again transforming as θ and ε, as shown in Fig. 1.

$$Q_{a_1} = \frac{1}{\sqrt{3}}(\Delta r_{12} + \Delta r_{13} + \Delta r_{23}).$$

$$Q_{e\vartheta} = \frac{1}{\sqrt{6}}(-2\Delta r_{23} + \Delta r_{12} + \Delta r_{13}).$$

$$Q_{e\varepsilon} = \frac{1}{\sqrt{2}}(\Delta r_{13} - \Delta r_{12}). \tag{6}$$

By appropriate substitutions the Hamiltonian matrix in Eq. 4 can easily be expressed in terms of the normal coordinates as:

$$H = \frac{k}{\sqrt{3}} \begin{pmatrix} 2Q_{a_1} & Q_{e\vartheta} & Q_{e\varepsilon} \\ Q_{e\vartheta} & -Q_{a_1} - \sqrt{2}Q_{e\vartheta} & \sqrt{2}Q_{e\varepsilon} \\ Q_{e\varepsilon} & \sqrt{2}Q_{e\varepsilon} & -Q_{a_1} + \sqrt{2}Q_{e\vartheta} \end{pmatrix}. \tag{7}$$

As this equation shows the a_1 and e orbitals depend oppositely on the totally symmetric coordinate. The genuine JT effect is encountered inside the e-shell, and is described by the lower

2×2 block of the Hamiltonian matrix. One has for this block:

$$H_{e\otimes e} = -\frac{k}{\sqrt{3}} Q_{a_1} \begin{pmatrix} 1 & 0 \\ 0 & 1 \end{pmatrix} + \frac{k\sqrt{2}}{\sqrt{3}} \begin{pmatrix} -Q_{e\vartheta} & Q_{e\varepsilon} \\ Q_{e\varepsilon} & Q_{e\vartheta} \end{pmatrix}. \quad (8)$$

In this equation, one observes the main ingredients of the JT effect. The potential depends on the totally symmetric mode, but both components vary in the same way with Q_{a_1}. Therefore, along this coordinate there is no splitting of the electronic degeneracy. On the potential energy hypersurface this coordinate forms a continuous seam where the two states cross. In contrast along the Q_e coordinates the degeneracy is split. The split eigenvalues can easily be obtained by diagonalizing the 2×2 JT matrix, yielding as roots:

$$E_{\pm} = -\frac{k}{\sqrt{3}} Q_{a_1} \pm \frac{k\sqrt{2}}{\sqrt{3}} \sqrt{Q_{e\vartheta}^2 + Q_{e\varepsilon}^2}. \quad (9)$$

This equation describes the typical conical intersection which is at the center of the well-known "Mexican hat"-type potential. On this potential, the degeneracy point at the origin is unstable, and the system will evolve on the minimal energy trough at the bottom of the Mexican hat. The coordinates of the Mexican hat may be rewritten in a polar form as:

$$Q_{e\vartheta} = \rho \cos \omega.$$
$$Q_{e\varepsilon} = \rho \sin \omega. \quad (10)$$

The pseudorotation in the ω-coordinate around the conical intersection corresponds to a rotational movement of the distortion itself. Along this path, the three nuclei rotate around their symmetry positions in a concerted way.[4] The waveform of the lowest root is expressed as:

$$|\psi_-\rangle = \cos\frac{\omega}{2} |\psi_{e\vartheta}\rangle - \sin\frac{\omega}{2} |\psi_{e\varepsilon}\rangle. \quad (11)$$

More elaborate forms of the potential can be constructed by including higher-order interaction terms, or by allowing for interactions between the e and a_1 orbitals.[5] The latter interaction can be described by the usual second-order perturbation theory, which was introduced by Fukui in reaction theories. In its simplest form one obtains:

$$E'_- = E_- - \frac{\langle\psi_-|H|\psi_{a_1}\rangle^2}{\Delta E}$$
$$= -\frac{k}{\sqrt{3}} Q_{a_1} - \frac{k\sqrt{2}}{\sqrt{3}} \rho - \frac{k^2\rho^2}{6\Delta E}(1 + \cos 3\omega). \quad (12)$$

The effect of this term will warp the intersection and delineate three directions with steeper descent where, for $k > 0$, one of the three bonds is compressed, forming an isosceles triangle.

The prototypal potential energy surface of the warped Mexican hat with three minima is of ubiquitous importance in chemistry. It dominates the structure and dynamics of hexacoordinated Cu^{2+} complexes, which display an $e \otimes e$ JT ground state.[6] This octahedral JT problem is isomorphic to the e-problem in trigonal symmetry. The three distortions correspond to the elongations of each of the three tetragonal axes of the octahedron.

This surface also occurs in chemical reaction theory and has been proposed to explain the stereospecific skeletal rearrangements of platinacyclobutane complexes. It was discovered by

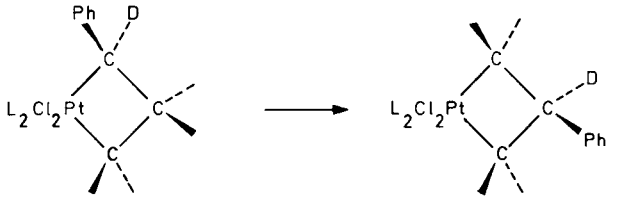

Scheme 1.

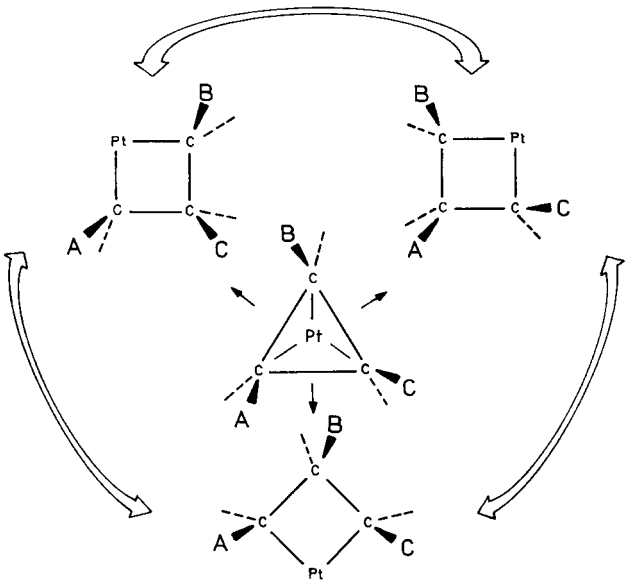

Fig. 2. Schematic view of the platinacyclobutane rearrangement mechanism. The structure in the centre is a triangular complex associated with a conical intersection. The circular trough around this intersection has minima at three cyclobutane complexes. The arrows indicate allowed interconversions, corresponding to even permutations of the carbon atoms with substituents A, B, and C [From: A. Ceulemans, *Polyhedron* **1991**, *10*, 1587].

Puddephatt et al.[7] that in these metallacycles a carbon in the α position, next to platinum, exchanges with a carbon in the β position. The simultaneous migration of both phenyl and deuterium substituents showed the permutational nature of the rearrangement, as indicated in the reaction scheme (Scheme 1).

Subsequent experiments demonstrated that the cyclobutane plane was retained during the reaction.[8] Wilker and Hoffmann[9] suggested that the rearrangement might be explained by an itinerary on the periphery of a so-called Jahn–Teller wheel around the degeneracy. This mechanism is shown schematically in Fig. 2. The symmetric origin of the surface consists of a triangular instability, and the minima are distorted structures formed by the motion of the metal towards one of the edges of the carbon triangle. Motion of the metal in the opposite sense, i.e. towards a corner of the triangle would yield a platinacyclopropyl type structure with an outer methylene bond. This structure sits as a saddle point between two permutational isomers of platinacyclobutane. We noted that out of six possible permutations of the three carbon atoms involved, only three actually occur when the system tunnels around in the Jahn–Teller trough.[10] These precisely correspond to the even permutations of the three substituents, as shown in Fig. 2.

The missing permutamers will constitute a similar Jahn–Teller merry-go-round process which is the optical antipode of the process depicted in Fig. 2. In other words, a reaction mechanism which proceeds on a Jahn–Teller surface is expected to be very highly stereoregular: it will not only preserve the orientation of the CH_2 groups with respect to the molecular plane, but also the handedness of the tricarbon structure. It is remarkable that almost thirty years after the experimental studies of this rearrangement by several teams, and fifteen years after the claims of the stereospecificity of the Jahn–Teller mechanism, the strict permutational order of the mechanism has not yet been demonstrated.

One may wonder to what extent orbital degeneracy is a vital aspect of this potential surface, where the reaction follows a path which may be far away from the symmetry origin where the degeneracy exists? In other words, does it matter to the reaction rate whether the central part of the surface is a local hill top, characteristic of a single-state problem, or a true conical intersection where two states meet? The prototypal surface of the former type is the so-called monkey's saddle, where three product valleys meet around a central local maximum.[11]

The surprising answer to this question is that no matter how far the actual reaction path is away from the intersection point, the conical intersection nevertheless makes its presence felt in the quantum dynamical properties of the system. This is a consequence of the fact that the electronic wave function, as described in Eq. 11 changes sign when transported adiabatically around the intersection. This phase effect was first noted by Longuet-Higgins[12] and is known as the Berry phase.[13] Its influence on reaction dynamics was demonstrated by careful studies of reaction rates and distributions of ideal systems such as the scattering of the hydrogen atom on the hydrogen molecule.[14]

Three-Fold Degeneracy: The Tetrahedron

The treatment of a triple degeneracy point proceeds in exactly the same way as before: now one takes as the basic structure the tetrahedron, which is the 3D congener of the triangle. The point group symmetry of the tetrahedron is T_d and this group is isomorphic to the symmetric group of four equivalent nuclei, S_4. The tetrahedron is also the smallest molecule which incorporates a triple degeneracy, and thus will exemplify the JT coupling for a t-state. As a basis, we consider now the set of four s-type functions on the vertices. They form a_1 and t_2 irreducible representations, corresponding to the scalar and the vector components of the familiar sp^3 hybrids:

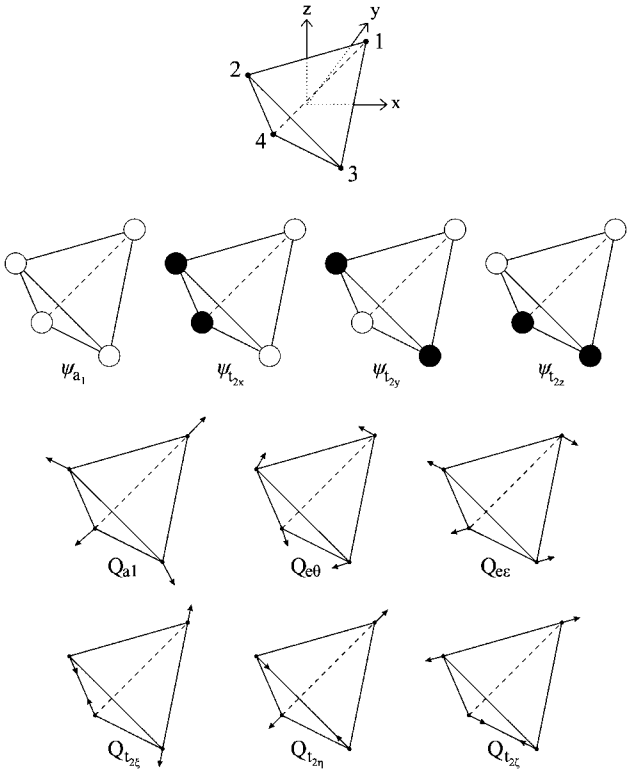

Fig. 3. The three-fold degeneracy and the tetrahedron: basic structure, orbital basis, and the normal modes corresponding to edge stretchings. The ψ_t-orbital basis is JT active under the Q_e- and Q_t-modes.

$$\psi_{a_1} = \frac{1}{2}(\varphi_1 + \varphi_2 + \varphi_3 + \varphi_4).$$
$$\psi_{t_2x} = \frac{1}{2}(\varphi_1 - \varphi_2 + \varphi_3 - \varphi_4).$$
$$\psi_{t_2y} = \frac{1}{2}(\varphi_1 - \varphi_2 - \varphi_3 + \varphi_4).$$
$$\psi_{t_2z} = \frac{1}{2}(\varphi_1 + \varphi_2 - \varphi_3 - \varphi_4). \quad (13)$$

These orbital combinations are shown schematically in Fig. 3. The interaction matrix in the orbital basis, ordered as $\{a_1, t_2x, t_2y, t_2z\}$ may be derived in exactly the same way as previously, and is shown below:

$$H = \frac{k}{2} \times \begin{pmatrix} \Delta r_{12} + \Delta r_{13} + \Delta r_{14} + \Delta r_{23} + \Delta r_{24} + \Delta r_{34} & \Delta r_{13} - \Delta r_{24} & \Delta r_{14} - \Delta r_{23} & \Delta r_{12} - \Delta r_{34} \\ \Delta r_{13} - \Delta r_{24} & -\Delta r_{12} + \Delta r_{13} - \Delta r_{14} - \Delta r_{23} + \Delta r_{24} - \Delta r_{34} & \Delta r_{34} - \Delta r_{12} & \Delta r_{23} - \Delta r_{14} \\ \Delta r_{14} - \Delta r_{23} & \Delta r_{34} - \Delta r_{12} & -\Delta r_{12} - \Delta r_{13} + \Delta r_{14} + \Delta r_{23} - \Delta r_{24} - \Delta r_{34} & \Delta r_{24} - \Delta r_{13} \\ \Delta r_{12} - \Delta r_{34} & \Delta r_{23} - \Delta r_{14} & \Delta r_{24} - \Delta r_{13} & \Delta r_{12} - \Delta r_{13} - \Delta r_{14} - \Delta r_{23} - \Delta r_{24} + \Delta r_{34} \end{pmatrix} \quad (14)$$

In a tetrahedron there are six edge bonds, giving rise to a six-dimensional coordinate space. This space can be organized in normal symmetry coordinates as follows:

$$Q_{a_1} = \frac{1}{\sqrt{6}}(\Delta r_{12} + \Delta r_{13} + \Delta r_{14} + \Delta r_{23} + \Delta r_{24} + \Delta r_{34}).$$

$$Q_{e\vartheta} = \frac{1}{\sqrt{12}}(-2\Delta r_{12} + \Delta r_{13} + \Delta r_{14} + \Delta r_{23} + \Delta r_{24} - 2\Delta r_{34}).$$

$$Q_{e\varepsilon} = \frac{1}{2}(-\Delta r_{13} + \Delta r_{14} + \Delta r_{23} - \Delta r_{24}).$$

$$Q_{t_2\xi} = \frac{1}{\sqrt{2}}(\Delta r_{13} - \Delta r_{24}).$$

$$Q_{t_2\eta} = \frac{1}{\sqrt{2}}(\Delta r_{14} - \Delta r_{23}).$$

$$Q_{t_2\varsigma} = \frac{1}{\sqrt{2}}(\Delta r_{12} - \Delta r_{34}). \quad (15)$$

Pictorial representations of these coordinates are given in Fig. 3. The interaction Hamiltonian in Eq. 14 can easily be expressed in these coordinates, giving rise to the following matrix expressions:

$$H = -\frac{k}{\sqrt{6}}Q_{a_1}\begin{pmatrix} -3 & 0 & 0 & 0 \\ 0 & 1 & 0 & 0 \\ 0 & 0 & 1 & 0 \\ 0 & 0 & 0 & 1 \end{pmatrix} + k\begin{pmatrix} 0 & \frac{1}{\sqrt{2}}Q_{t_2\xi} & \frac{1}{\sqrt{2}}Q_{t_2\eta} & \frac{1}{\sqrt{2}}Q_{t_2\varsigma} \\ \frac{1}{\sqrt{2}}Q_{t_2\xi} & \frac{1}{\sqrt{3}}Q_{e\vartheta} - Q_{e\varepsilon} & -\frac{1}{\sqrt{2}}Q_{t_2\varsigma} & -\frac{1}{\sqrt{2}}Q_{t_2\eta} \\ \frac{1}{\sqrt{2}}Q_{t_2\eta} & -\frac{1}{\sqrt{2}}Q_{t_2\varsigma} & \frac{1}{\sqrt{3}}Q_{e\vartheta} + Q_{e\varepsilon} & -\frac{1}{\sqrt{2}}Q_{t_2\xi} \\ \frac{1}{\sqrt{2}}Q_{t_2\varsigma} & -\frac{1}{\sqrt{2}}Q_{t_2\eta} & -\frac{1}{\sqrt{2}}Q_{t\xi} & -\frac{2}{\sqrt{3}}Q_{e\vartheta} \end{pmatrix}. \quad (16)$$

We observe the same opposite dependence on the totally symmetric stretching mode, which will separate the a_1 and t_2 shell. When the t_2-orbitals are partially occupied, a triplet JT effect arises, which will be of the form $t \otimes (e \oplus t_2)$, and is described by the lower 3×3 block in the interaction Hamiltonian of the preceding equation.

$$H_{t\otimes(e\oplus t_2)} = -\frac{k}{\sqrt{6}}Q_{a_1}\begin{pmatrix} 1 & 0 & 0 \\ 0 & 1 & 0 \\ 0 & 0 & 1 \end{pmatrix} + k\begin{pmatrix} \frac{1}{\sqrt{3}}Q_{e\vartheta} - Q_{e\varepsilon} & -\frac{1}{\sqrt{2}}Q_{t_2\varsigma} & -\frac{1}{\sqrt{2}}Q_{t_2\eta} \\ -\frac{1}{\sqrt{2}}Q_{t_2\varsigma} & \frac{1}{\sqrt{3}}Q_{e\vartheta} + Q_{e\varepsilon} & -\frac{1}{\sqrt{2}}Q_{t_2\xi} \\ -\frac{1}{\sqrt{2}}Q_{t_2\eta} & -\frac{1}{\sqrt{2}}Q_{t_2\xi} & -\frac{2}{\sqrt{3}}Q_{e\vartheta} \end{pmatrix}. \quad (17)$$

This is a particular form of the JT coupling matrix for a triple degeneracy. A more general form requires the use of different k's for e and t_2 modes. Eq. 17 describes a conical intersection in a five-dimensional coordinate space. The space contains three types of special directions, which preserve as much as possible the original tetrahedral symmetry.[15] In the subspace of the e-modes one encounters bisphenoidal distortions, corresponding to compression or elongation preserving D_{2d} symmetry. In the space of the t_2-modes one encounters trigonal distortions, again forming a compressed or elongated C_{3v} form. Finally, one also has butterfly modes, which consist of a mixture of the e- and t_2-modes, and which have only C_{2v} symmetry. In this case, only one of the bonds is either elongated (open butterfly) or compressed (closed butterfly). The subgroups that survive the JT distortion are the so-called epikernels of the coordinate space.[16] A detailed analysis of the symmetry breaking process in connection to the epikernel symmetries leads to the formulation of a general epikernel principle, which states that stationary points on a JT-surface will adopt epikernel, rather than kernel symmetries, and that higher ranking epikernels are preferred over lower ranking ones.[17]

Saturated tetrahedral clusters of transition-metals usually contain 60 valence electrons, as in the prototypal $M_4(CO)_{12}$ clusters, where M is a d^9 transition metal, such as Ni. Addition of one or two electrons leads to a t-type JT problem with the open-butterfly solutions, since typically one of the edge bonds is broken.[18]

In tetrahedral complexes of transition-metals one frequently observes D_{2d} or C_{3v} solutions. A very special case occurs in the $Fe(CO)_4$ fragment, which is obtained by photolysis of the 18-electron $Fe(CO)_5$ complex in a noble gas matrix.[19] The ground state of this cluster in a tetrahedral geometry has an open-shell structure with four electrons in the t_2-shell comprising the $\{d_{xz}, d_{yz}, d_{xy}\}$ orbitals. This configuration gives rise to a triplet t-state which is characterized by a potential energy surface with six C_{2v}-type local minima. The experiments of Poliakoff et al.[20] have shown that the isomers can be labeled isotopically by using $^{13}C^{18}O$. The possible "isotopomers" are shown in Fig. 4. A very specific reaction pattern emerges upon irradiation with IR lasers: the well known Berry rotation that would correspond to the concerted rearrangement of both axial and equatorial ligands is not observed. Instead the only allowed process is the non-Berry rearrangement where only one pair of ligands is exchanged. The occurrence of such stereospecificity points to the presence of a potential energy surface that is controlled by a JT origin. In the 5D distortion space of the $e \oplus t_2$ coordinates there are six C_{2v}-minima lying on a trough around the conical intersection. The reaction graph showing the pathways between the minima on this surface can be represented by an octahedron,[21,22] where the non-Berry

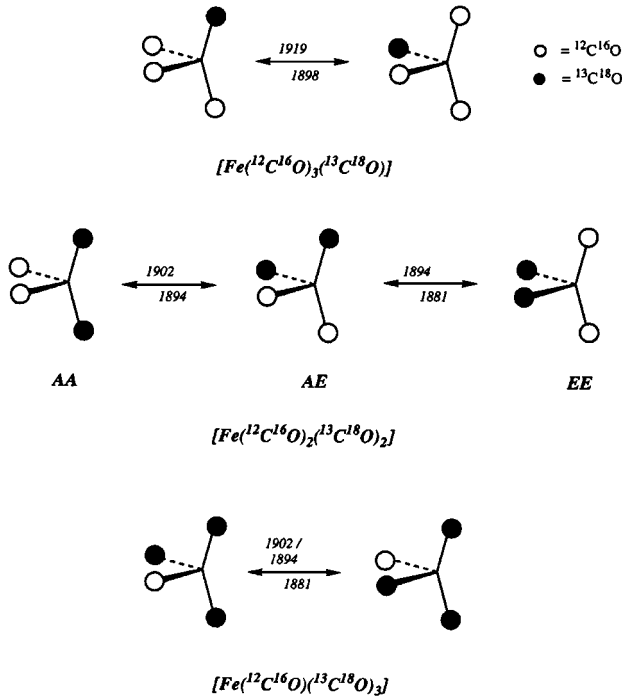

Fig. 4. Permutational isomerisations of the isotopically labeled $Fe(CO)_4$ fragment. The fragment has C_{2v} symmetry with two axial (A) ligands at an angle of 145° and two equatorial ones (E) at an angle of 120°. Selective IR-irradiations at the indicated wavenumbers cause permutations of axial and equatorial sites. Only non-Berry type rearrangements are observed [From: N. Leadbeater, *Coord. Chem. Rev.* **1999**, *188*, 35, redrawn from Ref. 20].

process forms the edges, as shown in Fig. 5. One should imagine that all the nodes of this reaction graph lie on a low-dimensional energy trough, rearrangements taking place via tunneling between the minima. Apparently IR irradiation of a given structure provides enough energy to provoke hopping to the nearest neighbour. However, on this surface, the Berry process would require two consecutive jumps to connect antipodal nodes on the octahedron, which is not likely to happen. Again the strict stereospecific relations between the minima and the existence of low-energy interconversion paths are indications for the important control that the Jahn–Teller effect can exert on chemical dynamics.

The proposed distortion octahedron connects six permutational isomers of a fully substituted ABCD tetrahedron, which is only half the number of possible isomers. As in the triangular case, we expect these twelve chiral isomers to be distributed over two independent JT-spheres that are each others mirror images. Experiments that would demonstrate this very special optical stereospecificity of the JT isomerisation mechanism are again still lacking.[10]

In molecules with octahedral symmetry the t-type degeneracy problem is entirely isomorphic to the tetrahedral case. Now the D_{2d} solutions correspond to the three tetragonal distortions, the C_{3v} solutions are D_{3d} and the C_{2v} solutions correspond to D_{2h} distortions. Such JT problems are less well documented than the e-types. In transition-metal complexes, t-type degeneracies usually originate from the t_{2g} shell, which has

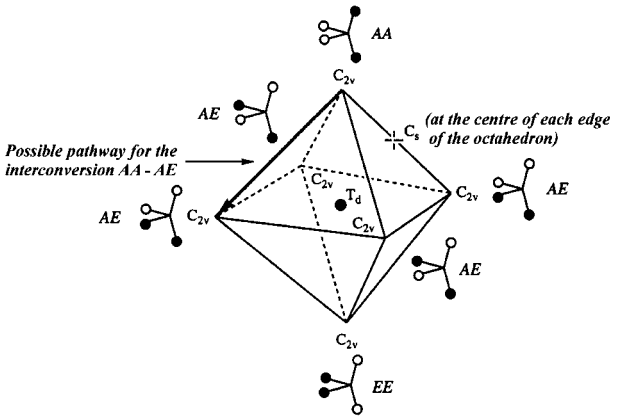

Fig. 5. Reaction graph in the form of an octahedron, showing the allowed non-Berry rearrangements paths, connecting C_{2v}-minima around a triple conical intersection [From: N. Leadbeater, *Coord. Chem. Rev.* **1999**, *188*, 35, redrawn from Ref. 21].

less bonding interactions than the e_g shell, and is thought to give rise to a smaller JT effect which is of a dynamic nature.[23] This ground level is characterized by a free rotation of the ligands on a distortion sphere surrounding their octahedral lodgings.[24] In icosahedral symmetry t-types degeneracies also occur. A notorious case is the anionic form of Buckminsterfullerene: the LUMO of C_{60} is of t_{1u}-symmetry, and various anionic open-shell states based on partial occupation of the three-fold degenerate orbital states are known.[25,26]

Four-Fold Degeneracy: The Pentahedroid

The icosahedral point group also allows for a four-fold degenerate orbital representation, which is usually denoted as the *g* representation. How can we understand the occurrence of such a degeneracy in a point group of 3D space, and how can we construct its JT matrix? The answer lies in the fact that the rotational subgroup of the icosahedron, commonly denoted as the group **I** with 60 elements, is isomorphic to the alternating group $\mathbf{A_5}$, which is the group of all even permutations of five objects, and is a halving subgroup of the symmetric permutation group S_5. This links the icosahedron to the symmetry of 4D space and suggests that we can simply extend our present construction procedure with one more dimension. So we end up in 4D space, the simplex of which is the pentahedroid. This is a hypertetrahedron, composed of five tetrahedra, in the same way as a tetrahedron is composed of four triangles.[27] A projection of this 4D object in 3D space is shown in Fig. 6. It corresponds to a centered tetrahedron, which is seen to consist of four tetrahedral cells surrounding the centre, the fifth cell being the outer tetrahedron itself. To show how the icosahedron can be embedded in this higher object, we remind that in a dodecahedron there are five inscribed cubes, as was already known to Euclid.[28] In Fig. 6 we provide the graph of a dodecahedron, with the labeling of the vertices. The five cubes will be denoted as *a*, *b*, *c*, *d*, *e*. They are defined by the following combinations of eight vertices:

$$\langle a\rangle = \{1, 9, 11, 18; 3, 10, 12, 20\}.$$
$$\langle b\rangle = \{2, 10, 15, 17; 4, 6, 11, 19\}.$$

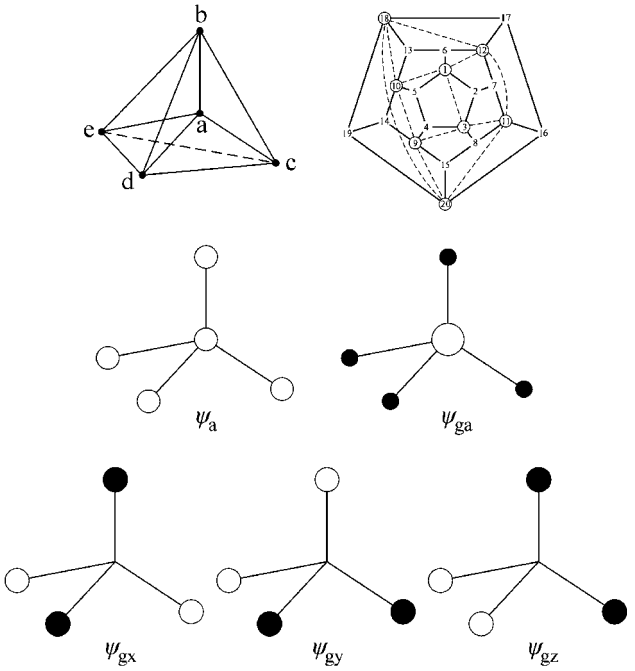

Fig. 6. The four-fold degeneracy and the hypertetrahedron. The centered tetrahedron (top left) represents a 3D projection of the hypertetrahedron. The drawing (top right) shows a Schlegel diagram of a dodecahedron. The eight connected nodes in this graph form one of the inscribed Euclid cubes, corresponding to vertex a in the hypertetrahedron. Also shown are the five orbital combinations transforming as a and g irreducible representations of the icosahedral symmetry group.

$$\langle c\rangle = \{3,6,14,16;5,7,15,18\}.$$
$$\langle d\rangle = \{4,7,13,20;1,8,14,17\}.$$
$$\langle e\rangle = \{5,8,12,19;2,9,13,16\}. \quad (18)$$

In this equation, we have divided the set of eight vertex labels into two subsets, corresponding to the two intertwined tetrahedra in each cube. The pentagonal rotations around the faces of the dodecahedron will permute the cubes among themselves. One can easily observe that there exists always a minimal rotation over $2\pi/5$ to connect any pair of cubes. In this way, all cubes may be said to be "equidistant." Hence, we can think of them as the five equidistant "vertices" forming the corners of the pentahedroid simplex of 4D space. We may denote five orbital components on these cubes, forming an orbital basis $\{\varphi_a,\varphi_b,\varphi_c,\varphi_d,\varphi_e\}$. Under the permutational group, S_5, these will give rise to a totally symmetric combination, and a four-fold degenerate orbital set, which we will denote as g-type:

$$\psi_a = \frac{1}{\sqrt{5}}(\varphi_a+\varphi_b+\varphi_c+\varphi_d+\varphi_e).$$
$$\psi_{ga} = \frac{1}{2\sqrt{5}}(4\varphi_a-\varphi_b-\varphi_c-\varphi_d-\varphi_e).$$
$$\psi_{gx} = \frac{1}{2}(-\varphi_b+\varphi_c-\varphi_d+\varphi_e).$$
$$\psi_{gy} = \frac{1}{2}(\varphi_b-\varphi_c-\varphi_d+\varphi_e).$$
$$\psi_{gz} = \frac{1}{2}(\varphi_b+\varphi_c-\varphi_d+\varphi_e). \quad (19)$$

These component symmetries, which are shown in Fig. 6, follow the standard symmetry conventions of Boyle and Parker,[29] which we have used throughout our work on icosahedral JT problems. As generators of the icosahedral group we have taken the five-fold rotation through the central $\langle 1,2,3,4,5\rangle$ face in the Schlegel diagram of Fig. 6, and the three-fold axis through vertex $\langle 1\rangle$. We made also use of the two-fold axis through the $\langle 4,5\rangle$ edge. These symmetry elements[30] act on the vertices of the pentahedroid in the following way:

$$\begin{aligned} C_5 &: a\to e\to d\to c\to b.\\ C_3 &: a\to a,\\ &\quad b\to c\to e,\\ &\quad d\to d.\\ C_2 &: a\to a,\\ &\quad b\to c,\\ &\quad d\to e. \end{aligned} \quad (20)$$

Armed with the symmetry orbitals we can set up the standard JT matrix for the simplex problem, adopting a contact term between the Euclid cubes in exactly the same way as before for the tetrahedral and triangular problems. The 4D simplex with 5 vertices has 10 bonds. In the parent group S_5, these transform as the direct sum of a totally symmetric representation, and a four-fold and five-fold degenerate representation. The four-fold and five-fold degenerate representation subduce respectively the g and h representation in the subgroup of the icosahedral rotations. Hence one has:

$$\begin{aligned} [(4,1)\otimes(4,1)] &= (5)\oplus(4,1)\oplus(3,2),\\ [\mathrm{g}\otimes\mathrm{g}] &= \mathrm{a}\oplus\mathrm{g}\oplus\mathrm{h}, \end{aligned} \quad (21)$$

where the first line refers to the irreducible representations of the symmetric group, and the second line contains the labels of the icosahedral rotation group. The square brackets denote that we are taking the symmetrized direct product. The corresponding symmetry adapted interaction coordinates are easily obtained. As an example the matrix element $\langle\varphi_{ga}|H|\varphi_{ga}\rangle$ can only contain the totally symmetric coordinate Q_a and the g-type component Q_{ga}. The former is the normalized sum of the ten edge stretchings, so that the latter can easily be obtained.

$$Q_a = \frac{1}{\sqrt{10}}(\Delta r_{ab}+\Delta r_{ac}+\Delta r_{ad}+\Delta r_{ae}+\Delta r_{bc}+\Delta r_{bd}+\Delta r_{be}+\Delta r_{cd}+\Delta r_{ce}+\Delta r_{de}).$$
$$Q_{ga} = \frac{1}{2\sqrt{15}}(-3\Delta r_{ab}-3\Delta r_{ac}-3\Delta r_{ad}-3\Delta r_{ae}+2\Delta r_{bc}+2\Delta r_{bd}+2\Delta r_{be}+2\Delta r_{cd}+2\Delta r_{ce}+2\Delta r_{de}).$$
$$Q_{gx} = \frac{1}{2\sqrt{3}}(\Delta r_{ab}-\Delta r_{ac}+\Delta r_{ad}-\Delta r_{ae}+2\Delta r_{bd}-2\Delta r_{ce}).$$
$$Q_{gy} = \frac{1}{2\sqrt{3}}(-\Delta r_{ab}+\Delta r_{ac}+\Delta r_{ad}-\Delta r_{ae}-2\Delta r_{be}+2\Delta r_{cd}).$$
$$Q_{gz} = \frac{1}{2\sqrt{3}}(-\Delta r_{ab}-\Delta r_{ac}+\Delta r_{ad}+\Delta r_{ae}+2\Delta r_{bc}-2\Delta r_{de}).$$

$$Q_{h\vartheta} = \frac{1}{2\sqrt{3}}(2\Delta r_{bc} - \Delta r_{bd} - \Delta r_{be} - \Delta r_{cd} - \Delta r_{ce} + 2\Delta r_{de}).$$

$$Q_{h\varepsilon} = \frac{1}{2}(\Delta r_{bd} - \Delta r_{be} - \Delta r_{cd} + \Delta r_{ce}).$$

$$Q_{h\xi} = \frac{1}{\sqrt{6}}(-\Delta r_{ab} + \Delta r_{ac} - \Delta r_{ad} + \Delta r_{ae} + \Delta r_{bd} - \Delta r_{ce}).$$

$$Q_{h\eta} = \frac{1}{\sqrt{6}}(\Delta r_{ab} - \Delta r_{ac} - \Delta r_{ad} + \Delta r_{ae} - \Delta r_{be} + \Delta r_{cd}).$$

$$Q_{h\zeta} = \frac{1}{\sqrt{6}}(\Delta r_{ab} + \Delta r_{ac} - \Delta r_{ad} - \Delta r_{ae} - \Delta r_{bc} + \Delta r_{de}). \quad (22)$$

Substitution of these values into the interaction matrix then provides the interaction Hamiltonian expressed in normal modes.[31] As before the totally symmetric and four-fold degenerate levels separate over the breathing mode. The four-fold JT Hamiltonian is then identified as the lower 4×4 block of the interaction matrix. It represents the coupling of the g-level with $g \oplus h$ vibrations.

$$H_{g\otimes(g\oplus h)} = kQ_a \begin{pmatrix} 1 & 0 & 0 & 0 \\ 0 & 1 & 0 & 0 \\ 0 & 0 & 1 & 0 \\ 0 & 0 & 0 & 1 \end{pmatrix} + \frac{k}{\sqrt{15}} \begin{pmatrix} 3Q_{ga} & -Q_{gx} & -Q_{gy} & -Q_{gz} \\ -Q_{gx} & -Q_{ga} & -\sqrt{5}Q_{gz} & -\sqrt{5}Q_{gy} \\ -Q_{gy} & -\sqrt{5}Q_{gz} & -Q_{ga} & -\sqrt{5}Q_{gx} \\ -Q_{gz} & -\sqrt{5}Q_{gy} & -\sqrt{5}Q_{gx} & -Q_{ga} \end{pmatrix}$$
$$+ \frac{k}{\sqrt{3}} \begin{pmatrix} 0 & \sqrt{5/2}Q_{h\xi} & \sqrt{5/2}Q_{h\eta} & \sqrt{5/2}Q_{h\zeta} \\ \sqrt{5/2}Q_{h\xi} & -Q_{h\vartheta} + \sqrt{3}Q_{h\varepsilon} & -1/\sqrt{2}Q_{h\zeta} & -1/\sqrt{2}Q_{h\eta} \\ \sqrt{5/2}Q_{h\eta} & -1/\sqrt{2}Q_{h\zeta} & -Q_{h\vartheta} - \sqrt{3}Q_{h\varepsilon} & -1/\sqrt{2}Q_{h\xi} \\ \sqrt{5/2}Q_{h\zeta} & -1/\sqrt{2}Q_{h\eta} & -1/\sqrt{2}Q_{h\xi} & 2Q_{h\vartheta} \end{pmatrix} \quad (23)$$

This matrix describes a conical intersection in the space of the interaction coordinates. For the present interaction model the coupling along the h-mode is dominant and yields a trigonal distortion of D_{3d} symmetry. Since the icosahedron has 10 trigonal directions, there will be 10 equivalent trigonal minima. It is possible to define interaction potentials for which the g-mode becomes the dominant active mode. In this case, the JT activity develops along a tetrahedral distortion mode favoring one of the Euclid cubes, with point group symmetry T_h. In this case, there will be five equivalent minima, at equal distances from each other.[31]

The JT effect of a four-fold degenerate state has not yet been documented but model systems are already available, and the first experimental manifestations may soon be discovered. The parent cluster of the fullerene class, C_{20}, is a dodecahedral structure with a four-fold degenerate HOMO of g_u-symmetry occupied by two electrons. Both this cluster and its cationic form are expected to show JT activity, which may, however, be small since the HOMO is in principle a non-bonding orbital. Calculations predict this cage to be stable,[32] but so far there is only elusive evidence for the existence of this cluster in the gas phase.[33] A more interesting candidate is the C_{80} icosahedral fullerene.[34] This may be looked upon as a special descendant of the C_{20} parent, obtained by chamfering all edges,[35] as shown in Fig. 7. This special type of extension leads again to an open-shell structure with two electrons in a four-fold degenerate orbital set, this time, however, of the gerade g_g-type. A most interesting manifestation of this four-fold degenerate HOMO is the existence of the stable endohedral $La_2@C_{80}$ complex.[36] The incorporated lanthanide ions in this structure are trivalent, meaning that the cage has accepted six electrons to become a C_{80}^{6-} fulleride. This is a closed shell structure due to the complete filling of the g-shell. One can speculate that removal of one electron in this case will lead to JT activity of the g-type, coupled to the cylindrical symmetry of the La dimer inside the cage.

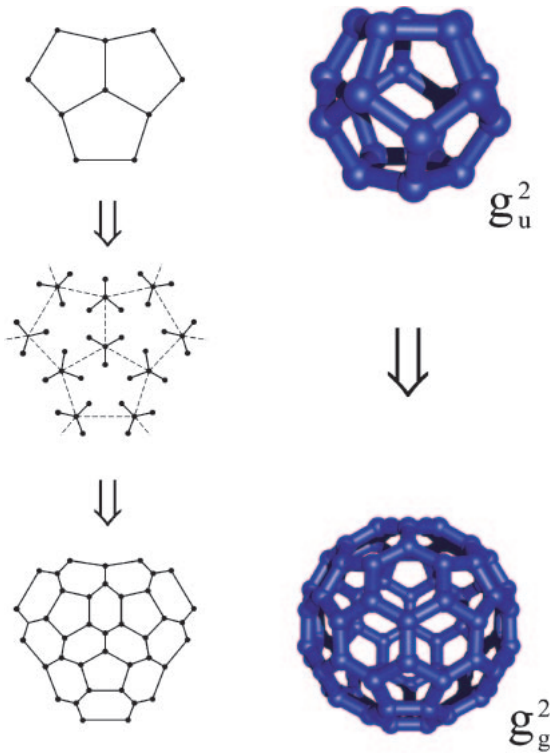

Fig. 7. Two icosahedral carbon cages with a four-fold degenerate HOMO. In C_{20} (top), the HOMO has g_u-symmetry and is occupied by two electrons. The chamfering operation shown on the left, is a cage extension which replaces all edges by hexagons and multiplies the number of atoms by a factor of 4. It turns C_{20} into C_{80}. The degeneracy of the HOMO is kept, but the parity is changed from odd to even.

Five-Fold Degeneracy: The Complete Graph K6

The highest orbital degeneracy that can be realized by spatial symmetry is the five-fold degenerate irreducible representation h in molecules with icosahedral symmetry. Buckminsterfullerene itself has a bonding HOMO of h_u type and is thus expected to show this type of JT activity in its cationic form. If we want to understand this case from the same point of view as we have treated all other degeneracies, we find ourselves forced to take one more step into higher dimension and consider the case of a 5D space, the simplex of which can be symbolized by the complete graph of 6 nodes, denoted in graph theory as $\mathbf{K_6}$. Its symmetry group is the permutation group of six elements. As before the set of the six vertices contains one scalar, which is the totally symmetric combination, and one 5-dimensional vector, which forms the basis of our orbital h-representation. How can we now construct these vector components in such a way that they obey the standard symmetry rules, which define the $\vartheta, \varepsilon, \xi, \eta, \zeta$ components of the h-representation?

This question really concerns the connection between the abstract group S_6 and the group of icosahedral rotations, which is isomorphic to $\mathbf{A_5}$. In other words, can we identify in an icosahedron an orbit of six structures which are permuted among themselves by the symmetry operations, and are equidistant from each other? The answer to this question will not only yield a systematic way to construct the Jahn–Teller Hamiltonian, but also gives a deeper insight into the mere existence of five-fold degeneracies in an icosahedron. Clearly such structures indeed exist. They simply constitute the set of the six pentagonal axes in the icosahedral frame. So the twelve pentagonal faces in a dodecahedron can be arranged in six pairs of antipodal faces, forming a set of six interlaced pentagonal antiprisms. Each pentagonal direction is surrounded by the five-other directions, and for this reason the six pentagonal directions are all nearest neighbours. They thus constitute the set of six objects that are permuted among themselves by the symmetry elements of the icosahedron. These permutations characterize the group of the rotations of an icosahedron as a special subgroup of the symmetric group S_6. We will label the six pentagonal directions by capital letters as follows:

$$\begin{aligned}
\langle A\rangle &= \{1,2,3,4,5;16,17,18,19,20\}.\\
\langle B\rangle &= \{1,2,7,12,6;9,15,20,19,14\}.\\
\langle C\rangle &= \{2,3,8,11,7;10,14,19,18,13\}.\\
\langle D\rangle &= \{3,4,9,15,8;6,13,18,17,12\}.\\
\langle E\rangle &= \{4,5,10,14,9;7,12,17,16,11\}.\\
\langle F\rangle &= \{5,1,6,13,10;8,15,20,16,11\}.
\end{aligned} \tag{24}$$

For each pentagonal direction the vertex labels denote the upper and lower pentagonal faces of the corresponding pentagonal antiprism. The action of the icosahedral operators on these six elements gives rise to the following permutations:

$$\begin{aligned}
C_5 &: A \to A,\\
&\quad F \to E \to D \to C \to B.\\
C_3 &: A \to B \to F,\\
&\quad C \to D \to E.
\end{aligned}$$

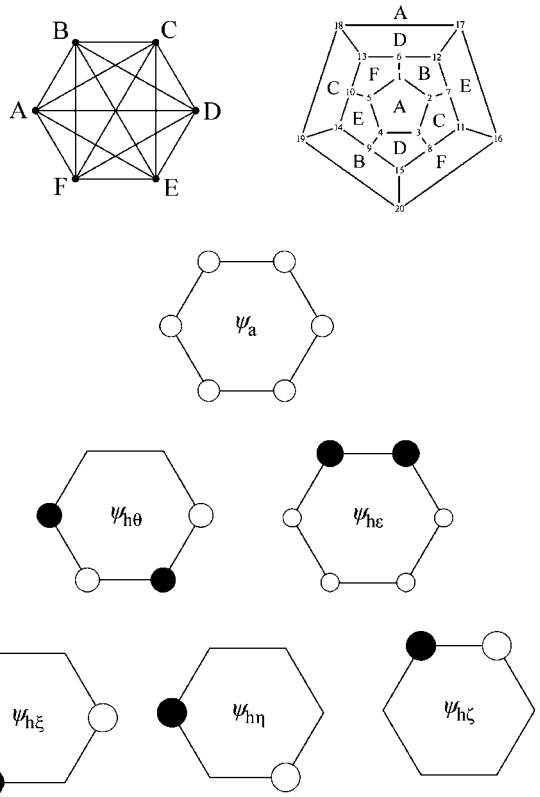

Fig. 8. The five-fold degeneracy and the complete graph $\mathbf{K_6}$. The nodes of the graph are identified by the six pentagonal directions, as listed in Eq. 24. The six orbital combinations on these nodes transform as a and h irreducible representations of the icosahedral symmetry group.

$$\begin{aligned}
C_2 &: A \to E,\\
&\quad F \to D,\\
&\quad B \to B,\\
&\quad C \to C.
\end{aligned} \tag{25}$$

We can now easily derive the set of basis orbitals, which are adapted to the icosahedral symmetry. As before this set divides into a totally symmetric "all bonding" component, and a remaining five-fold degenerate representation which is the fundamental "vector" of our 5D space, as shown in Fig. 8.

$$\begin{aligned}
\psi_a &= \frac{1}{\sqrt{6}}(\varphi_A + \varphi_B + \varphi_C + \varphi_D + \varphi_E + \varphi_F)\\
\psi_{h\vartheta} &= \frac{1}{2}(-\varphi_A + \varphi_D - \varphi_E + \varphi_F)\\
\psi_{h\varepsilon} &= \frac{1}{\sqrt{12}}(\varphi_A - 2\varphi_B - 2\varphi_C + \varphi_D + \varphi_E + \varphi_F)\\
\psi_{h\xi} &= \frac{1}{\sqrt{2}}(\varphi_D - \varphi_F)\\
\psi_{h\eta} &= \frac{1}{\sqrt{2}}(-\varphi_A + \varphi_E)\\
\psi_{h\zeta} &= \frac{1}{\sqrt{2}}(-\varphi_B + \varphi_C)
\end{aligned} \tag{26}$$

With these basisfunctions and using the same mechanical procedure as before, it is again straightforward to construct an

Table 1. Embedding of the Icosahedral Rotation Group (**I**–**A**$_5$) in the Symmetric Group of Order 6, S_6[a)]

S_6	1 (1^6)	15 (1^4,2)	40 (1^3,3)	45 (1^2,2^2)	90 (1^2,4)	120 (1,2,3)	144 (1,5)	15 (2^3)	90 (2,4)	40 (3^2)	120 (6)
A$_5$	E			15 C_2			12 C_5 12 $C_5{}^2$			20 C_3	
(6)	1	1	1	1	1	1	1	1	1	1	1
(5,1)	5	3	2	1	1	0	0	−1	−1	−1	−1
(4,2)	9	3	0	1	−1	0	−1	3	1	0	0

a) The irreducible representations (6), (5,1), (4,2) subduce a, h, g+h resp.

interaction matrix and extract the Jahn–Teller part. There will be 15 edge bonds inside the 5D simplex, giving rise to one totally symmetric breathing mode, and 14 JT coordinates. These give rise to the standard $h \otimes (g \oplus 2h)$ JT-Hamiltonian.[37] Since the present Hamiltonian has a special S_6 symmetry, we will obtain a high-symmetry form of the Hamiltonian where the g-mode and one of the h-modes belong to the same permutational representation. In Table 1, we provide the subduction relations between the symmetric group and the icosahedral rotations. A more elaborate analysis of the group-theoretical aspects of this connection will be deferred to a separate publication.

From the chemical point of view the JT effect in a five-fold degeneracy can give rise to several kinds of distortions. The main minimal energy solutions have pentagonal or trigonal symmetry. The pentagonal solutions, with D_{5d} symmetry, are entirely situated in the 5D space of the h-modes, and indeed form six equidistant minima. The reaction graph which connects these minima is therefore indeed the **K**$_6$ graph, on which our analysis was based. Depending on the coupling parameters the system may also show a preference for trigonal solutions, with D_{3d} symmetry. In this case the minima are extended in $g \oplus h$ space, and form a set of ten equivalent minima, which are, however, not all equidistant. These ten minima correspond to the ten triangular faces in the 5D simplex. Several papers have been devoted to the interesting topology of this surface,[38,39] which may give rise to different dynamic ground states,[40,41] depending on the strengths of the trigonal coupling constants.

The Jahn–Teller Theorem

In this paper, we have attempted to present the universal structure of all JT cases in finite point groups, using the power of the symmetric groups. The procedure started from the concept of a degenerate basis set. Such a set of dimension n may always be viewed as the fundamental vector in a simplex of $N = n + 1$ vertices, where all components are interacting with all others. This simplex can be realized with point-like objects in n-dimensional space. The doublet, triplet, quartet, and quintuplet degeneracies are thus visualized by simplexes in 2-, 3-, 4-, and 5-dimensional space. In the symmetric group S_N describing the symmetry of the simplex, the N vertices provide a basis for a totally symmetric scalar and a fundamental irreducible vector representation, which in the standard notation are denoted as (N) and $(N-1,1)$ respectively. We will denote this splitting as follows:

$$\Gamma_N = \Gamma_1 + \Gamma_n. \tag{27}$$

Now we let all equidistant vertices interact with each other. The N nodes, give rise to $N(N-1)/2$ edge bonds, which together form the coordinate space. The symmetry of the stretchings along these bonds can be obtained as follows:

$$\begin{aligned}\Gamma_{\Delta r} &= [\Gamma_N]^2 - \Gamma_N \\ &= [\Gamma_1 + \Gamma_n]^2 - \Gamma_N \\ &= \Gamma_1 + \Gamma_n + [\Gamma_n]^2 - \Gamma_N \\ &= [\Gamma_n]^2. \end{aligned} \tag{28}$$

The first line in this expression states that the symmetry of the stretching modes is obtained by taking the symmetrized square of the vertex representation, and subtracting the diagonal elements which also transform as the vertex representation. The result in Eq. 28 states that the symmetry of the active modes exactly coincides with the symmetrized square of the irreducible representation of the degeneracy level. This square contains the totally symmetric representation and the irreducible representations of the JT active modes. This result shows that the coordinate space of the simplex will exactly contain the active modes that are required to break the symmetry. It provides a simple rationale of the JT theorem based on a symmetric group analysis of degenerate representations in the point groups.[42] From the symmetry point of view the interaction coordinates are formed by all cross-products of the basic orbitals.

Conclusion

The occurrence of degeneracies is a typical quantum aspect of molecular nature, and as such is intimately connected to molecular structure and reactivity, both in gaseous phase and in solution. Chemistry abounds with manifestations of vibronic instability of degeneracies, be it as genuine symmetry cases described in the Jahn–Teller effect, or derivative cases as in non-symmetrical conical intersections which are mainly studied in relation to photochemical reactivity.[43,44] The present account did not aim to give a full overview of the known cases, but rather attempted to show their common roots, which are connected to dimensionality. A chemical perspective was developed which draws attention to geometry and structure. The symmetric groups of complete graphs are seen to provide a uniform group-theoretical basis. This approach complements the usual physical perspective which starts from the rotational invariance **SO(n)** groups of the electronic manifold.[45] In principle we can also envisage a further extension of this symmetric group treatment which will provide the rationale for the observation that the JT effect does not really destroy the electronic degeneracy but rather replaces it by a vibronic one of the same kind.[46]

The account would be incomplete, without mentioning the proverbial exceptions that confirm the strength of the JT effect as a universal rule. We know at least three cases where the claims of instability are overruled by more powerful symmetries: i) cylindrical symmetries in linear molecules, a case which was already known from the beginning by Jahn and Teller,[1] ii) time reversal symmetry which gives rise to the well known Kramers degeneracy in odd-electron systems, iii) and last but not least the quasi-spin symmetry which is a characteristic of the structure of half-open shells and follows from particle-hole equivalence.[47,48]

The authors thank the Flemish Government for continuing support through the concerted action scheme. E. L is a postdoctoral fellow of the Flemish National Science Foundation FWO. In 2002, A. C. received a fellowship of the Japan Society for the Promotion of Science and was hosted by prof. N. Kobayashi from Tohoku University. Fruitful collaborations with N. Kobayashi, T. Sato, and T. Kato are gratefully acknowledged.

References

1 H. A. Jahn, E. Teller, *Proc. R. Soc. London* **1937**, *A161*, 220.

2 The JT effect in chemistry and physics is described in several monographs. See e.g.: a) R. Englman, *The Jahn–Teller Effect in Molecules and Crystals*, Wiley-Interscience, London, **1972**. b) I. B. Bersuker, V. Z. Polinger, *Vibronic Interactions in Molecules and Crystals*, Springer, New York, **1989**. c) I. B. Bersuker, *The Jahn–Teller Effect*, Cambridge, Cambridge University Press, **2006**.

3 An analogy may be found in a triangle of anti-ferromagnetically coupled spins, see: A. I. Popov, V. I. Plis, A. F. Popkov, A. K. Zvezdin, *Phys. Rev. B: Condens. Matter* **2004**, *69*, 104418.

4 T. Sato, L. F. Chibotaru, A. Ceulemans, *J. Chem. Phys.* **2005**, *122*, 054104.

5 R. Meiswinkel, H. Köppel, *Chem. Phys.* **1990**, *144*, 117.

6 M. A. Hitchman, W. Maaskant, J. van der Plas, C. J. Simmons, H. Stratemeier, *J. Am. Chem. Soc.* **1999**, *121*, 1488.

7 R. J. Al-Essa, R. J. Puddephatt, M. A. Quyser, C. F. H. Tipper, *J. Am. Chem. Soc.* **1979**, *101*, 364.

8 C. P. Casey, D. M. Scheck, A. J. Shusterman, *J. Am. Chem. Soc.* **1979**, *101*, 4233.

9 C. N. Wilker, R. Hoffmann, *J. Am. Chem. Soc.* **1983**, *105*, 5285.

10 A. Ceulemans, *Polyhedron* **1991**, *10*, 1587.

11 R. E. Stanton, J. W. Mc Iver, *J. Am. Chem. Soc.* **1975**, *97*, 3632.

12 H. C. Longuet-Higgins, *Proc. R. Soc. London* **1975**, *A344*, 147.

13 M. V. Berry, *Proc. R. Soc. London* **1984**, *A392*, 45.

14 S. C. Althorpe, *J. Chem. Phys.* **2006**, *124*, 084105.

15 I. B. Bersuker, V. Z. Polinger, *Sov. Phys. JETP* **1974**, *39*, 1023.

16 P. Murray-Rust, H.-B. Bürgi, J. D. Dunitz, *Acta Crystallogr., Sect. A* **1979**, *161*, 220.

17 A. Ceulemans, L. G. Vanquickenborne, *Struct. Bonding* **1989**, *71*, 125.

18 A. Ceulemans, *J. Chem. Phys.* **1986**, *84*, 6442.

19 M. Poliakoff, J. J. Turner, *Angew. Chem., Int. Ed.* **2001**, *40*, 2809.

20 B. Davies, A. Mc Neish, M. Poliakoff, J. J. Turner, *J. Am. Chem. Soc.* **1977**, *99*, 7573.

21 M. Poliakoff, A. Ceulemans, *J. Am. Chem. Soc.* **1984**, *106*, 50.

22 A. Ceulemans, D. Beyens, L. G. Vanquickenborne, *J. Am. Chem. Soc.* **1984**, *106*, 5824.

23 P. L. W. Tregenna-Piggott, H. P. Andres, G. J. Mc Intyre, S. P. Best, C. C. Wilson, J. A. Cowan, *Inorg. Chem.* **2003**, *42*, 1350.

24 B. R. Judd, in *Vibronic Processes in Inorganic Chemistry*, ed. by C. D. Flint, NATO Advanced Science Institutes Series, Kluwer, Dordrecht, **1989**, Vol. C288, p. 79.

25 T. Kodama, M. Kato, K. Mogi, M. Aoyagi, T. Kato, *Mol. Phys. Rep.* **1997**, *18–19*, 121.

26 A. Auerbach, N. Manini, E. Tosatti, *Phys. Rev.* **1994**, *B49*, 12998.

27 N. B. Backhouse, P. Gard, *J. Phys. A* **1974**, *7*, 2101.

28 A. Ceulemans, P. W. Fowler, M. Szopa, *Math. Proc. R. Ir. Acad.* **1998**, *98A*, 139.

29 L. L. Boyle, Y. M. Parker, *Mol. Phys.* **1980**, *39*, 95. In the appendix of this reference, the second element in the third row of the C5 matrix for T1 should read $-1/2$.

30 These generators correspond to the C5, C3, and C2 generator axes used in Ref. 29.

31 A. Ceulemans, P. W. Fowler, *Phys. Rev. A: At., Mol., Opt. Phys.* **1989**, *39*, 481.

32 P. R. Taylor, E. Bylaska, J. H. Weare, R. Kawai, *Chem. Phys. Lett.* **1995**, *235*, 558.

33 H. Prinzbach, F. Wahl, A. Weiler, P. Landenberger, J. Wörth, L. T. Scott, M. Gelmont, F. Sommer, B. von Issendorff, *Chem. Eur. J.* **2006**, *12*, 6268.

34 K. Nakao, N. Kurita, M. Fujita, *Phys. Rev. B: Condens. Matter* **1994**, *49*, 11415.

35 R. B. King, M. V. Diudea, *J. Math. Chem.* **2006**, *39*, 597.

36 S. Nagase, K. Kobayashi, T. Akasaka, *Bull. Chem. Soc. Jpn.* **1996**, *69*, 2131.

37 A. Ceulemans, P. W. Fowler, *J. Chem. Phys.* **1990**, *93*, 1221. The drawings labeled as Fig. 3 in this paper are erroneous. Figure 3a should be replaced by the drawing of the Petersen graph, and Figure 3b by its complement.

38 E. Lijnen, A. Ceulemans, *Adv. Quantum Chem.* **2003**, *44*, 183.

39 E. Lijnen, A. Ceulemans, *Phys. Rev. B: Condens. Matter* **2005**, *71*, 014305.

40 C. P. Moate, M. C. M. O'Brien, J. L. Dunn, C. A. Bates, Y. M. Liu, V. Z. Polinger, *Phys. Rev. Lett.* **1996**, *77*, 4362.

41 N. Manini, P. De Los Rios, *Phys. Rev. B: Condens Matter* **2000**, *62*, 29.

42 For a proof of the JT theorem, based on the point groups, see: E. Ruch, A. Schönhofer, *Theor. Chim. Acta* **1965**, *3*, 291. See also Ref. 24.

43 L. Blancafort, M. A. Robb, *J. Phys. Chem. A* **2004**, *108*, 10609.

44 *Conical Intersections*, ed. by W. Domcke, D. R. Yarkony, H. Köppel, Advanced series in Physical Chemistry, World Scientific, New Jersey, **2004**, Vol. 15.

45 A. Ceulemans, *J. Chem. Phys.* **1987**, *87*, 5374.

46 *Vibronic Interactions in Molecules and Crystals*, Springer, New York, **1989**, pp. 195–196.

47 A. Ceulemans, *Top. Curr. Chem.* **1994**, *171*, 27.

48 E. D. Savage, G. E. Stedman, *Adv. Quantum Chem.* **2003**, *44*, 21.

Arnout Ceulemans (born in Antwerpen, Belgium, 1952) is full professor of Theoretical Chemistry at the University of Leuven, Belgium. He received his Ph.D. in Leuven while working in the group of Prof. Vanquickenborne on theoretical models for ligand field photochemistry. In 1984, he was laureate of the Royal Belgian Academy of Science, and habilitated in 1986 with a thesis on the Jahn–Teller effect in complexes and clusters. He was a postdoctoral fellow of Carleton University (Ottawa), and recipient of the Stanley Kipping Fellowship of the University of Nottingham. In 2002, he was awarded the JSPS Fellowship for research in Japan. His research interests are the application of group-theoretical and topological methods at the border between chemistry and physics. He is vice-chairman of the Leuven Institute for Nanoscale Physics and Chemistry, INPAC.

Erwin Lijnen (born in Heusden, Belgium, 1979) graduated in chemistry at the University of Leuven. In 2005, he recieved his Ph.D. while working in the group of Prof. Ceulemans on the polyhedral state of molecular structures and processes. He is currently holding a postdoctoral fellowship of the Fund for Scientific Research-Flanders (FWO) at the University of Leuven where he is working on the topological representation of molecular structures. His research interests are in the area of mathematical chemistry, mainly on the use of combinatorial and topological methods in molecular sciences.